UNIVERSIDAD POLITÉCNICA DE MADRID
E.T.S. AERONÁUTICA Y DEL ESPACIO
⊢ M.Sc. Aeronautical & Astronautical Engineering ⊣

Statistical Characterization of Biomimetic Gecko Adhesives

Pedro Rivero Ramírez
(M.Sc. Student) – pedro.rivero.ramirez@alumnos.upm.es

Chicago, July 2018

Advisors: Matthew Spenko (Ph.D. Faculty) & Aiva Simaite (Ph.D. Faculty)

This paper presents a way to characterize the adhesion of biomimetic grippers developed with NASA/JPL technology. These grippers emulate the adhesion forces present in geckos' fingertips, so they are capable of sticking temporarily without any preconditioning of the surface (e.g. velcros) and keeping it intact. They also do not need of any concrete environment to work –unlike vacuum grippers that require some sort of atmosphere– which makes them specially useful for space purposes such as for robots capable of climbing the outer surface of a space vehicle in order to perform inspections or repairs. High voltage electrostatic fields are applied for adhesion enhancement. A statistical method for characterizing the effects on adhesion of surface roughness will be developed based on the concept surface defects. In particular, controlled defects on grippers themselves will be statistically analyzed through a sample of over 2,000 experiments; matching the measured defects with the statistical results. Through this process the validity of the statistical analysis will lead to a way of predicting surface defects without performing any direct measurements of them. Then, the dual problem will be considered to extend the analysis from relative differences in adhesion over different faulted grippers to relative differences in adhesion over different substrates. This way, the effects of surface roughness on the adhesion of the grippers will be characterized without need of a yet intractable direct measurement. Because this method does not require substrates to have any specific surface conditions, its use might be extended to study adhesion on more challenging surfaces such as kapton thermal covers which often appear on space vehicles.

0. Introduction

This section introduces the essentials of gecko adhesives, work that has already been done, and fabrication methods. The choice of configuration for the adhesives, as well as the main goal of this study are also presented here for the first time. It based on [1] – from which one illustrative figure has been borrowed –, and its only purpose is to contextualize the work done, which will be discussed in upcoming sections.

0.1. Gecko Adhesives

There are a number of techniques to achieve adhesion between two surfaces. Some of them tend to perform well on a specific surface type, but fail when applied to a different one. An example of these kind of adhesives are the so called controllable adhesives; for instance those based on suction [2], microstructured (i.e. fibrillar, gecko-like, dry) [5], electromagnets [3], or microspines [4]. The first two kinds mentioned work well on smooth surfaces, but fail on rough ones.

In the case of micro-structured adhesives, which we will be dealing with, surface roughness can prevent the adhesive from engaging with the substrate. This is an important issue, as something as slight as the texture left behind from a paint roller can induce huge effects.

Previous work has made use of a combination of electrostatic and microstructured adhesives [1, 6] in an effort to achieve a method that is applicable to both smooth and rough surfaces. The resulting adhesive has been proven to outperform the sum of its individual parts on many surfaces [6], and has potential in a variety of applications that range from manufacturing [7] to satellite grappling in space [12], perching micro air vehicles [10,11], and mobile robots capable of climbing inverted surfaces [8,9]. The configuration used in this paper will consist of one of the electrodes being solid, and the other one on a different layer forming parallel stripes (see Fig. 1).

Surface roughness characterization still presents a problem towards confidently determining the actual adhesive force/pressure presented over a certain substrate. This paper introduces a tentative statistical method to characterize the effects of surface roughness, which is verified through its equivalent dual problem of determining controlled surface defects on the gecko-adhesives.

0.2. Background

Both electrostatic adhesion and micro-structured fibrillar adhesion have been utilized for this work. We will now briefly describe previous work done in these areas both alone and combined in order to provide with background for the rest of the paper.

0.2.1. Electrostatic adhesives

A major gain with electrostatic adhesion is that it can be applied to almost any substrate regardless of its conducting or non-conducting nature. Due this fact, electrostatic adhesion is especially applicable to space environments where ferromagnetic materials are uncommon, pressure sensitive adhesives out-gas, and suction does not work due to the lack of an atmosphere. For electrostatic adhesion, we create an electrostatic field by producing a high voltage potential (typically on the order of kV) across dielectric-embeded electrodes. This manifests as an adhesive force [13]: on conductive surfaces due to electrons forming electron-holes under the negative electrodes, and on non-conductive surfaces, due to the electric field polarizing the substrate's molecules [14].

A variety of factors such as the voltage potential, insulator thickness, electrode geometry (e.g. width, gap spacing, pattern), and substrate permittivity relate to the magnitude of the electrostatic adhesion force. Increasing the voltage potential or substrate permittivity, as well as decreasing the gap size between electrodes or the insulator thickness, improves adhesion force [14].

For this paper, the electrostatic adhesives will be manufactured by sandwiching electron patterns chemically edged between kapton layers, yielding a highly compliant electrostatic adhesive pad with an overall thickness of approximately 400 μm, and high surface friction properties. This allows the pad to conform to micro-rough surfaces and create a large real-area of contact.

0.2.2. Microstructured adhesives

For the last fifteen years, several manufacturing techniques have been developed in order to fabricate artificial micro-structured adhesives [16]. For this study, we utilize asymmetric, or directional, micro-structured hairs. These produce a high real area of contact when loaded in a preferred direction [18]. Whenever this load is released, the adhesives are capable of detaching from the surface presenting near zero force.

0.2.3. Combination of electrostatic and microstructured adhesives

Previous work in the field [1, 6] shows how a micro-structured dry adhesive element can be molded directly into the contact surface of an electrostatic adhesive, so that the electrostatic adhesive can provide a normal adhesion force which pre-loads the micro-structured adhesive and helps adapt the entire adhesive to the surface. Only a handful of research groups have actually created such adhesives.

0.3. Fabrication Method

For this work, we will use a fabrication process which comes from a number of previous papers [1,15, 20, 21] to manufacture the employed adhesives. To be more specific, we cast a micro-structured adhesive directly onto a previously fabricated electrostatic adhesive.

As it has already been stated, a directional microstructured adhesive was used for this work. Tests were done under shear loading, although some light weights were used to ensure different degrees of normal pre-attachment between the substrate and the adhesive. The electrostatic force enhances the normal adhesion, which in turn improves the shear load required to disengage the adhesive from the substrate. As sown in [1], using a directional adhesive results in extremely high shear loads, blending in the effects of the electrostatic adhesive and the microstructured adhesive. This will allow us to double the number of valid experiments under a fixed amount of adhesives by simply testing with the electrodes both ON/OFF.

The electrostatic adhesive was fabricated by bonding a cover layer of Kapton film onto a copper-clad Kapton film, Pyralux, patterned with the desired electrode geometry. As for the hybrid adhesive, the fibrillar structures could also be put closer to the electrodes. The vertical separation between electrodes and fibrillar stalks with this approach was only that of the Kapton film thickness: $25 \mu m$.

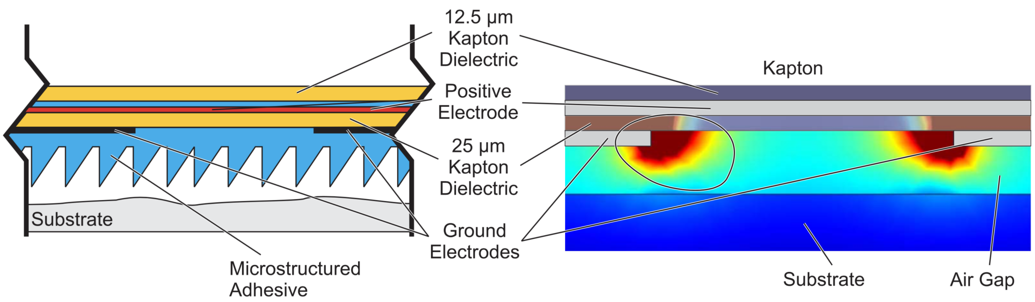

Figure 1: (Left) The layered design introduced in [1] attempts to decrease the gap size by putting the positive and ground electrodes on separate planes, and utilizing a dielectric layer with a high dielectric voltage break- down strength (Kapton). (Right) Cross-section of the electric field strength simulation results using this design. Drawn to scale. **Reference** [1].

The electrode geometry was created using a chemical etching process. A mask of the electrode pattern was printed, then toner transferred directly onto the copper-clad Kapton, Pyralux AC, and finally, the resulting piece was etched using Ferric Chloride. Both gap and width of the electrodes after etching were not exactly as designed, since the etching process is not exact. Based on observations from [1] the electrode gap size after etching was typically up to $50 \mu m$ greater than the nominal size.

The fabrication process was:

1. **Chemically etch the electrode pattern** onto a $25 \mu m$ thick Kapton film with $9 \mu m$ of copper cladding.
2. **Place a strip of the bonding resign along and edge**. This is used both as the insulator and an adhesive to bond the Kapton layers together.
3. **Place the plain Kapton film on the resin**.
4. **Roll the resin out to all the edges** using a $200g$, $31mm$ diameter cylindrical roller to create a consistent thickness of approximately $10 \mu m$. This process is necessary to prevent the entrapment of air bubbles, which could provide paths for electrical shorts as well as to provide a thin and even resin layer.
5. **Place the pad in an oven** at 140°C for $4h$ to fully cure the resin.
6. **Mold the micro-structured adhesives onto the surface**, as described in [6].

1. Experiments & Results

This section introduces the experiments which have been conducted, equipment that was used, and the results obtained from them.

1.1. Equipment

There are three main distinct pieces of equipment to tell apart each experiment. These are: **substrates**, **adhesive pads**, and **weights** laying on top of the pads. The measuring device will be configured in the same manner for all experiments, so it will not add any variability from one experiment to another.

1.1.1. Substrates

Experiments were conducted using several types of substrates, varying their dielectric constant and surface roughness. An overview them can be found in Table 1.

1.1.2. Adhesive Pads

Different types of adhesives varying in composition were used. In order to improve properties of the microstructured adhesive, two main additives were added to the polymer in different proportions: CuPc and Starch. CuPc gives a blueish tone to the polymer used to mold the gecko microstructures on, which will prove useful for testing the later proposed characterization method; as the coloring allows for visual inspection of the gecko-adhesive's surface. Notice too, that adhesives with and without CuPc should not really be compared with each other. Table 2 shows a quick overview of all relevant properties of adhesives of all the different compositions.

1.1.3. Weights

Normal pre-attachment shows a great influence over the adhesive shear force registered on each experiment, which is consistent with [1, 6]. Due to the scale of the microstructures, it became harder to ensure a same level of pre-attachment on every measurement, specially on smooth surfaces. This led to huge variability in the results, with the corresponding standard deviations being too big to accept any comparative results.

SUBSTRATE	Dielectric ($\epsilon_r \simeq$)	Rghn.#0 (μm)	Rghn.#1 (μm)	Rghn.#2 (μm)
Glass	7.5	0.01 ± 0.005	–	–
Acrylic	4.0	–	0.95 ± 0.1	–
Polypropylene	1.6	0.78 ± 0.05	1.25 ± 0.05	1.92 ± 0.1
MDF	1.1	5.61 ± 0.7	–	–

Table 1: Substrate properties used for the conducted experiments. The given dielectric constants are estimations based on a number of different popular charts.

TYPE	CuPc % Wt.	Starch % Wt.	# Samples
# 1	0.0	0.0	2
# 2	4.0	1.0	2
# 3	4.0	5.0	2

Table 2: Adhesive compositions and number of samples employed.

In order to reduce the impact of normal pre-attachment on the measurements, light weights ($5g$ except in subsection §1.2.2) were used on top of the gecko-adhesives. This method ensured that the adhesives had a similar level of pre-attachment over different experiments, increasing the chances of reproducing similar results. Instead of applying the weight right on top of the adhesive, a small MDF block was placed in between to ensure an even distribution of the weight across the entire surface of the adhesive pad.

1.2. Experiments

In order to characterize the behavior of the gecko-adhesives several experiments were performed measuring the adhesive shear force of the pads, and grouped them by type. Each type of experiment was designed to evaluate different aspects of these adhesives, and together, they could be used for our larger statistical purposes. The behavior of the adhesives was analyzed laying different weights on top of them, as well as turning the electrostatic adhesion ON ($5000V$) and OFF ($0V$). In the end, a total of over 2000 valid tests were run.

1.2.1. Electrostatic Adhesion

According to [1], adding an electric field to the pad results in electrostatic adhesion, which increases the normal pressure, and consequently improves the microstructral adhesion to shear stresses. Therefore, such increase on different materials was to be searched for. We tested the type #3 adhesives on the four roughest substrates we had: Acrylic, Polypropylene (roughness #1 and #2) and MDF. Results are shown in Fig. 2.

MDF showed the lowest shear pressure values, but the biggest relative increase when electrostatic adhesion is turned ON. This might be due to the internal structure of MDF being made out of different grains with lots of interfaces between one another; in contrast with the other materials which form more of a continuous medium. As a matter of fact, it is difficult to tell apart experiments with and without the electrostatic field for all the non-MDF substrates. Later on some possible causes for this which will motivate the statistical analysis that we will use to characterize surface roughness will be analyzed. By telling apart measurements made with different adhesive samples, correction for differences between those samples will be possible, which will lead to obtaining more precise results where the electrostatic effects are much better appreciated.

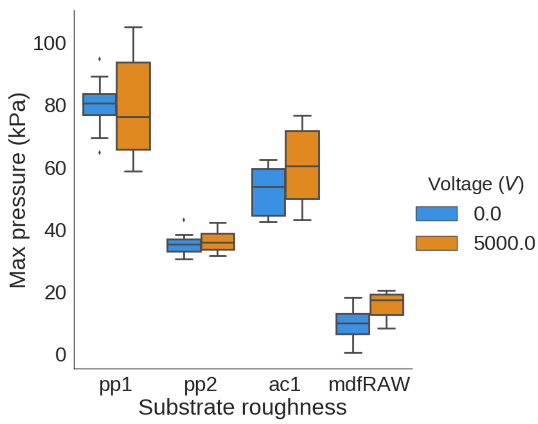

Figure 2: Maximum shear pressure on different substrates for type #3 adhesives, with electrostatic adhesion turned ON ($5000V$) and OFF ($0V$).

The dual problem where adhesive samples are no longer needed to be told apart, but rather substrate samples, will conform the roughness characterization method proposed by this study. The validity of the method will be based in the validity of its counterpart (efficiently separating measurements from different adhesive samples), which can be demonstrated much more easily by means of empirical observations correlated with statistical results.

1.2.2. Weight Curve

On top of ensuring normal pre-attachment, weights were also used to analyze how normal force influences adhesion, as well as what happens when electrostatic adhesion was added.

Moreover, this turns out to be interesting in order to characterize the effective normal pressure induced by the electrostatic field. The following weights ere used: $5g$, $10g$, $20g$, $30g$, $40g$, $50g$, $70g$, $80g$, and $100g$.

As it was shown in the previous subsection, the substrate which shows a greater increase when electrostatics are added is MDF, and so that will be the one used here. For adhesive type #3 sample #1, the results are shown in Fig. 3. According to the experiments, turning electrostatics ON ($5000V$) the extrapolation to $0g$ weight is equivalent to a weight of about $63g$ with electrostatics OFF. Therefore, the normal force generated by the electrostatic field is, in this case, approximately $0.62N$ over a reference surface area of $322mm^2$; which is equivalent a normal pressure of $1.92kPa$.

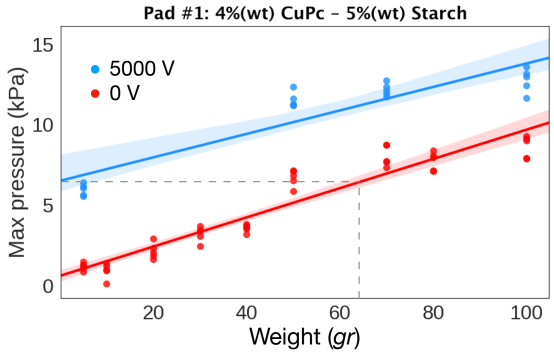

Figure 3: Weight curve showing results of max shear pressure vs applied weight with electrostatics both ON/OFF for adhesive type #3 sample #1.

In order to observe the qualitative behavior in more detail, when measuring for adhesive type #1 sample #1, the setup of the experiment was also changed. This makes the quantitative comparison of both experiments meaningless, but enhances slope deviations in the weight curves with electrostatics both ON/OFF. This way, it was determined that both lines are not parallel but rather closing in on one another as depicted in Fig. 4. Such observation was uncertain in the previous case due to the confidence intervals obtained when performing a linear regression over the results.

1.3. Statistical Experiment Set-Up

As it was introduced before in subsection §1.2.1, the difference between electrostatics ON and OFF for all non-MDF substrates (see Fig. 2) could not be told. The working hypothesis was that, because of manufacturing imprecision, the adhesive samples differed significantly from one another, with the resulting increase in error. To check this hypothesis, samples for adhesives type #1 and #2 were picked showing significant differences between one another on either their effective surface (this could only be done for adhesives with some amount of CuPc, as we mentioned in subsection §1.1.2), or their results in experiments. One fairly good sample, and one fairly bad one were chosen.

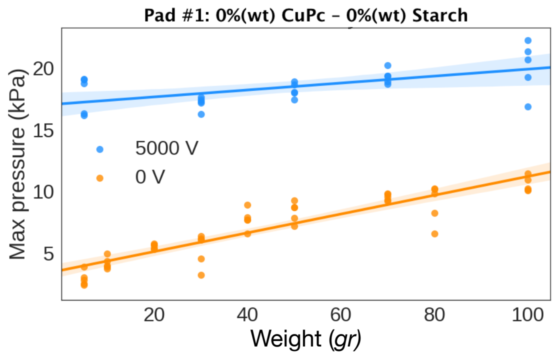

Figure 4: Weight curve showing results of max shear pressure vs applied weight with electrostatics both ON/OFF for adhesive type #1 sample #1.

Fig. 6 shows the results obtained from experiments on every non-MDF substrate and for all adhesive types, which are distinguished by Starch concentration: notice though, that type #1 adhesives have 0% CuPc as well as 0% Starch, in contrast with the 4% CuPc on the other adhesive types.

As expected, there is a great overlap between measurements with and without the electrostatic field, being adhesive type #3 the least affected one. This is due to the choice of samples for the other two types of adhesives. The goal was to statistically correct the faulted sample so that its measurements can be compared with those from the good one. If the process works, a much significant separation between results with and without electrostatic adhesion was expected – due to the decrease in the standard deviation of the measurements. Then, this method could be used for both enhancing the results, and determining from them the defects on certain samples. The dual problem will consist on telling from experiment the effective surface "defects" on certain substrates, which will stand as a **characterization of their surface roughness**.

The defects found on the faulted samples can be evaluated by visual inspection if the sample has some amount of CuPc. This can be used for contrast with the statistical results. These defects on a scanning electron microscope, *SEM* for short, can be seen Fig. 5.

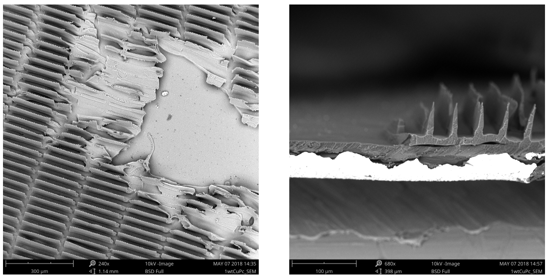

Figure 5: Defects on sample #2 of type #2 adhesive seen under a scanning electron microscope.

2. Analysis & Characterization

This section presents the proposed method of characterization in detail, and analyses its validity using an easier to verify equivalent problem. How to move from the studied case to the one of interest will be explained, which should be a fairly straight forward process as it can be understood as a dual problem. It also introduces a corrected version of Fig. 6 and explains why the success of this process can be understood as confirmation that the characterization method works. Finally, a characterization method for electrostatic adhesion is introduced as well.

2.1. Sample Normalization

It was previously introduced the hypothesis that, due to manufacturing errors, merging the results from two different samples of the same adhesives leads to significant standard deviations. To fix this, instead of merging the results directly, a previous normalization will be performed, then they will be merged and finally de-normalized to get back to the domain of interest. This way, typical discrepancies will be filtered out mathematically, resulting in clear mean differences that different adhesive samples of identical composition show when tested under the same circumstances (see Fig. 7).

Some examples of how different samples have different effective surface area will be showed in subsection §2.2 (see Fig. 8). Further discrepancies may be consequence of inappropriate repetitiveness in the preparation of experiments due to factors such as normal pre-attachment; or because of errors introduced by the electrode manufacturing. Therefore, this will result in three different merging processes to unify the data from different samples: **Direct merge**, normalization merge with de-normalization using the **average mean** of the samples, and normalization merge with de-normalization using the **maximum mean** of the samples.

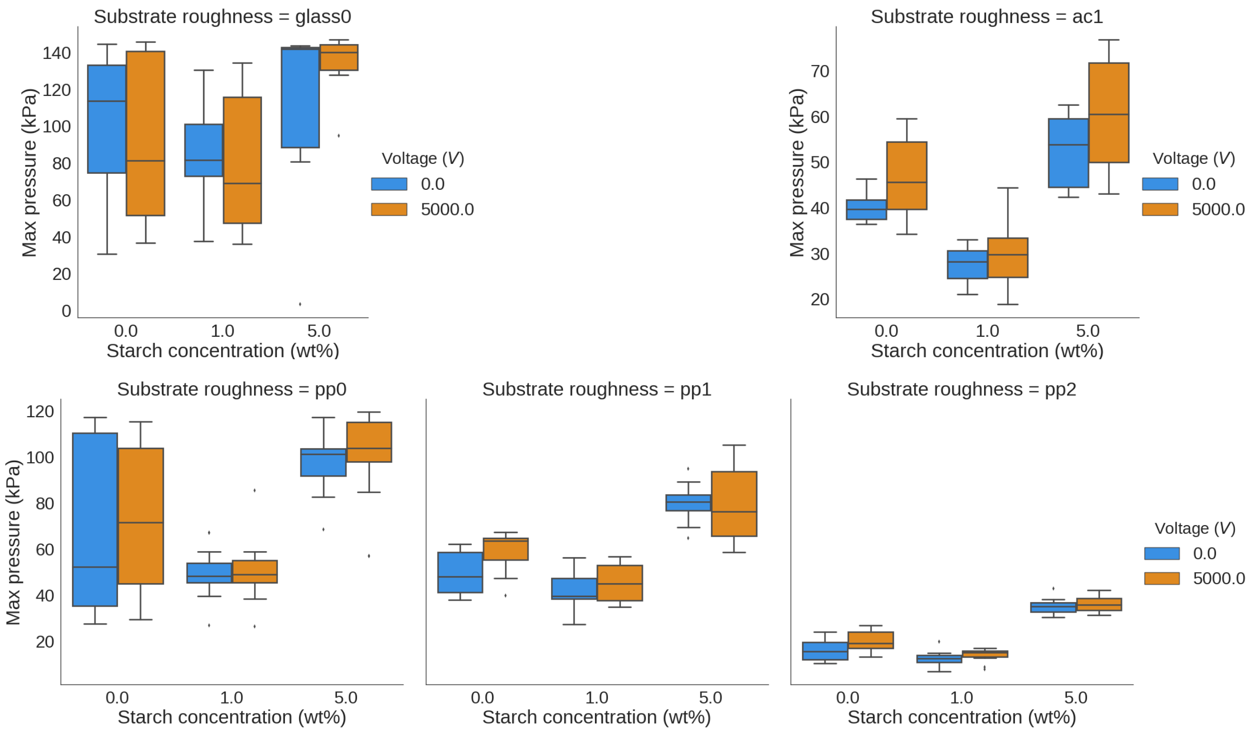

Figure 6: Results on every non-MDF substrate for adhesive types #1, #2, and #3 with and without electrostatics. Notice that adhesive type #1 has 0% CuPc as well as 0% Starch.

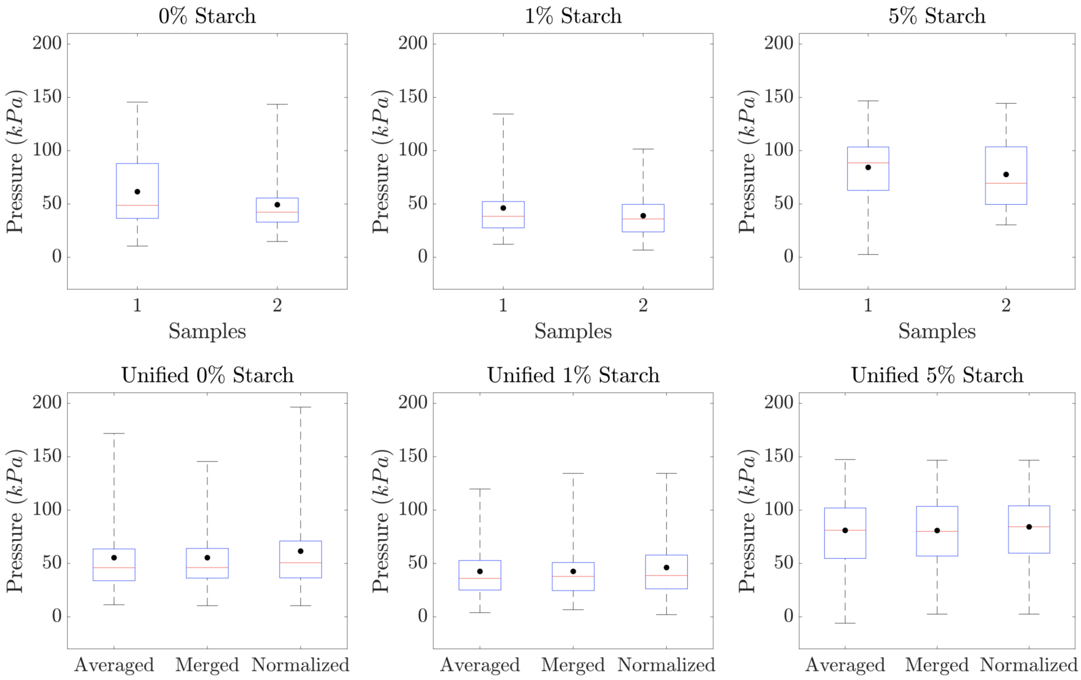

Figure 7: Unified distributions for each set of samples and merging method: **Averaged** (normalized to average mean), **Merged** (Direct Merge), **Normalized** (Normalized to the maximum mean).

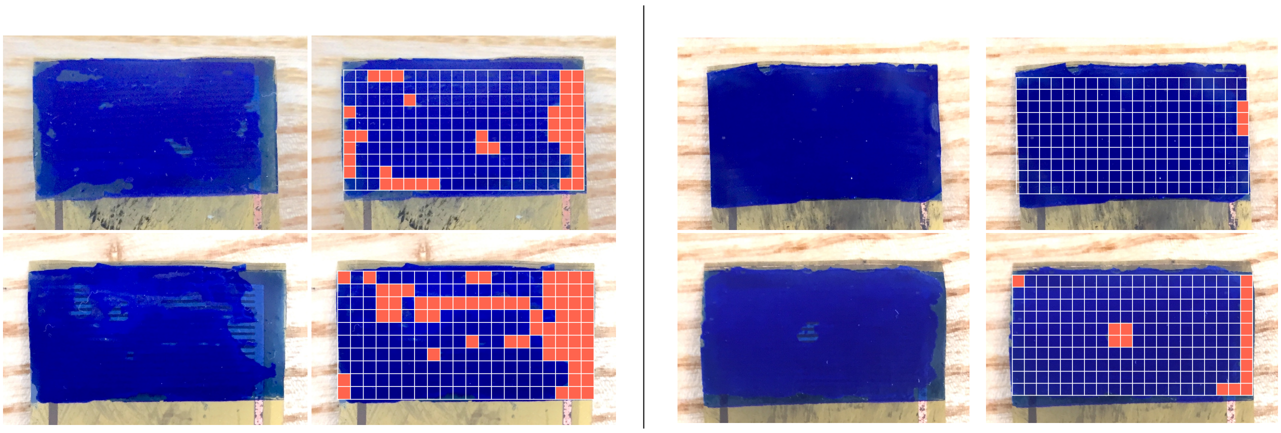

Figure 8: Difference in effective adhesive surface between two samples by visual inspection. (Left) Type #2 samples. (Right) Type #3 samples.

Calling μ the mean value of a sample's measurements and σ its standard deviation, the Gaussian normalization formula will be:

$$X_{norm} = \frac{X - \mu}{\sigma} \tag{2.1}$$

Where, according to Bessel's correction and calling the number of measurements N, an unbiased estimator for the variance is given by:

$$\sigma_j^2 = \frac{1}{N-1}\sum_{i=1}^{N}(x_i - \mu_j)^2 \tag{2.2}$$

Calling the number of samples for each kind of pad S, and given that the distributions being merged are independent from one another (covariances equal zero), the standard deviation for the merged data can be approximated in the following way:

$$\sigma^2_{merged} = \frac{N-1}{S \cdot N - 1} \sum_{j=1}^{S} \sigma_j^2 \simeq \frac{1}{S} \sum_{j=1}^{S} \sigma_j^2 \tag{2.3}$$

Which will allow to de-normalize the unified data by inverting equation (2.1) once a new mean (μ) is picked from the two given options (average or maximum mean).

Notice that it was assumed $\mu_j = \mu \, \forall j$, given that we will impose this condition during de-normalization; as well as $N \gg 1$, where there were the same amount of measurements N on every sample. This formula is not valid to compute the variance of the direct merge, as in that case $\exists \mu_j \neq \mu$ and so equation (2.3) would be illegal.

A special case where this formula is valid would be when merging the normalized distributions ($\mu_j = \mu = 0$ and $\sigma_j = 1 \, \forall j$). This yields:

$$\sigma^2_{merged} = \frac{1}{S} \sum_{j=1}^{S} (1) = 1 \tag{2.4}$$

In other words, the merging of normalized distributions results in another normalized distribution given that all of the initial ones have the same amount of elements $N \gg 1$.

Of course, the mean of the merge can be found as follows:

$$\mu = \frac{1}{S \cdot N} \sum_{j=1}^{S} N \cdot \mu_j = \frac{1}{S} \sum_{j=1}^{S} \mu_j \tag{2.5}$$

So if $\mu_j = \mu_k \, \forall \{j,k\}$, then $\mu = \mu_j \, \forall j$. See in Fig. 7 how the unified distribution looks for each set of samples and merging method.

In order to correct the defects of a faulted sample, normalization to the maximum mean will be used, which is the method corresponding to the best manufactured sample.

2.2. Effective Surface Calculation

From this process of normalization to the maximum mean, a way of inferring the surface defects out of the statistical results is found. First, assume that given a certain microstructure adhesive composition the pressure that any sample made out of it is capable to sustain will be the same. Therefore:

$$P \equiv \frac{F_j}{S_j} \quad \Rightarrow \quad \frac{F_1}{S_1} = \frac{F_2}{S_2} \quad \Rightarrow \quad \frac{S_2}{S_1} = \frac{F_2}{F_1} \tag{2.6}$$

$$\Rightarrow \quad \frac{\Delta S}{S_1} = 1 - \frac{F_2}{F_1} \tag{2.7}$$

Now, taking averages:

$$\langle \frac{\Delta S}{S_1} \rangle = 1 - \langle \frac{F_2}{F_1} \rangle = 1 - \langle F_2 \rangle \langle \frac{1}{F_1} \rangle \tag{2.8}$$

Due to the fact that measurements on one sample do not affect measurements in the other ($\mathrm{Cov}(F_1, F_2) = 0$). And thanks to **Jensen's inequality** this is:

$$\langle \frac{\Delta S}{S_1} \rangle \geq 1 - \frac{\langle F_2 \rangle}{\langle F_1 \rangle} \tag{2.9}$$

Giving a **conservative approach** (not overestimating) to figure out the percentual surface defects on the less effective sample. Introducing the mean values in this formula it yields:

$$\langle \frac{\Delta S}{S_1} \rangle \Big|_{0\%\text{Starch}}^{\textbf{(Statistics)}} \geq 19.88\%$$
$$\langle \frac{\Delta S}{S_1} \rangle \Big|_{1\%\text{Starch}}^{\textbf{(Statistics)}} \geq 15.70\%$$
$$\langle \frac{\Delta S}{S_1} \rangle \Big|_{5\%\text{Starch}}^{\textbf{(Statistics)}} \geq 7.87\%$$

Now, it is possible to check how accurate these results are by visual inspection of the pads. This can only be done for the cases where there is some amount of CuPc, as the resulting coloring is key to distinguishing the affected areas. In order to perform the visual inspection pictures of the pads were taken and meshed, marking the regions of the mesh where significant defects are found (see Fig. 8). This method, although very simple, will prove to be hugely effective, resulting in the following percentual surface defects:

$$\langle \frac{\Delta S}{S_1} \rangle \Big|_{1\%\text{Starch}}^{\textbf{(Visual)}} \simeq 15.00\%$$
$$\langle \frac{\Delta S}{S_1} \rangle \Big|_{5\%\text{Starch}}^{\textbf{(Visual)}} \simeq 7.11\%$$

These seem to be great results. Nevertheless, notice that the results from visual inspection are less than the lower bound determined by the statistics. This is most likely due to other factors different from surface defects such as inappropriate repetitiveness in the preparation of experiments due to factors such as pre-attachment; or because of errors introduced by the electrode manufacturing. There is also an error introduced by the visual inspection method which would have to be accounted for, and that might result in a slight increase in the results found.

By introducing these surface corrections, it is found that all three merging methods are pretty much equivalent – as depicted in Fig. 9. Finally, if correcting the results shown in Fig. 6 as to account for surface defects and plotting them, it is found that, as it was previously announced, the electrostatic effects are more pronounced and more easily spotted (see Fig. 10). These results point towards validating the beneficial effects of adding electrostatic adhesion to the gecko-adhesives, over a wider range of substrates than it was previously considered in papers such as [1, 6, 7].

2.3. Roughness Characterization

In theory, roughness affects adhesion as it produces a decrease in the effective contact surface. Adapting our now "proved" method of statistical analysis to determine the percentage drop in effective surface when changing from one roughness to another. This is the dual problem to the one of adhesive surface defects; therefore, it is based upon the same equations.

$$\langle \frac{\Delta S}{S_1} \rangle \geq 1 - \frac{\langle F_2 \rangle}{\langle F_1 \rangle} \tag{2.10}$$

Which gave a conservative estimate of the effective surface defects. These effective surface defects will now be on the substrate and will characterize its roughness. The duality plays as follows:

- **Adhesive Surface Defects**: Same substrate, different adhesive samples of the same composition.
- **Roughness**: Different substrates of the same composition, same adhesive sample.

2.4. Characterization of Electrostatic Effects

Using the weight curves introduced in subsection §1.2.2 the adhesive behavior of the pads when some voltage is applied can be studied, and related to the standard measurements without any voltage.

It was already shown that, due to the **monotonic growth** of the weight curves with and without electrostatics (see Fig. 3), there is a *bijection* between the values in one case and the other; this is, there is a one to one relation from shear loads with electrostatics and some weight, to a case with a certain – generally different – weight an no applied voltage. Specially, there is a unique equivalent value of weight associated to the case where we have some applied voltage but no weight. This is an ideal way to characterize the electrostatic effects in terms of the normal adhesion they generate (see [1]), which relates to an empirical, easy to determine equivalent applied weight.

Also, drawing the **distance between the two weight curves as a function of weight**, and studying what happens when the curves intersect (if they ever do) is now another possible technique. This will imply studying the *seemingly* linear relation between applied weight and measured shear force; and could potentially lead to explaining why it appears that electrostatics have so little effect when the shear loads are already big without any voltage on the electrodes.

3. Final Conclusions & Prospective Work

Experimental results point towards an increase of about $10 - 20\%$ in shear adhesive pressure due to activating the electrostatic adhesion with a voltage potential of $5kV$. This is not as much as it was predicted by previous research, but still presents an important gain in adhesion which could be further augmented.

Although the results are not conclusive yet, they glance at least two possible ways to characterize gecko-adhesives related phenomena:

- **Roughness Characterization**: In terms of an effective contact surface associated to the different roughness on a substrate.
- **Characterization of Electrostatic Effects**: Using weight curves.

For validation of both methods they will have to be tested on a number of different scenarios. Some of them are: more roughness kinds (e.g. directional roughness), more substrates (wider range of dielectric constants and different morphologies), more pad compositions, different voltages, and asymptotic behavior. Also the visual inspection method could be improved to try to narrow down the effectiveness of the statistical evaluation. This would strengthen the case for the proposed roughness characterization method.

As for the characterization of electrostatic effects, weight curves show an easy, yet promising way of studying the induced normal pressure and its effects on shear adhesion.

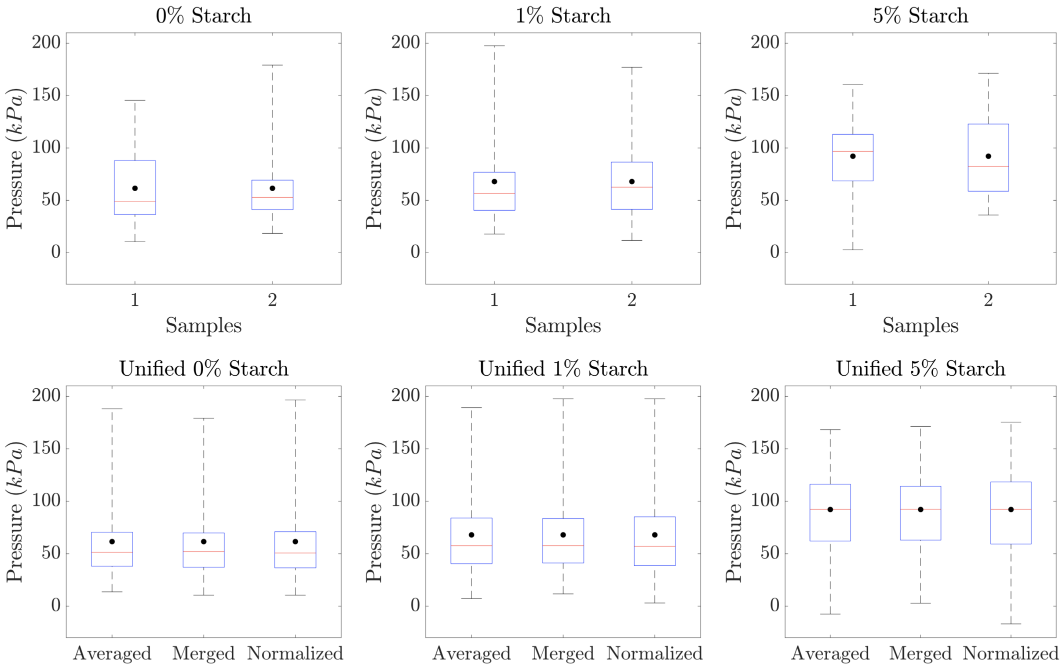

Figure 9: Unified distributions for each set of samples and merging methods after performing the statistical surface correction: **Averaged** (average mean), **Merged** (Direct Merge), **Normalized** (maximum mean).

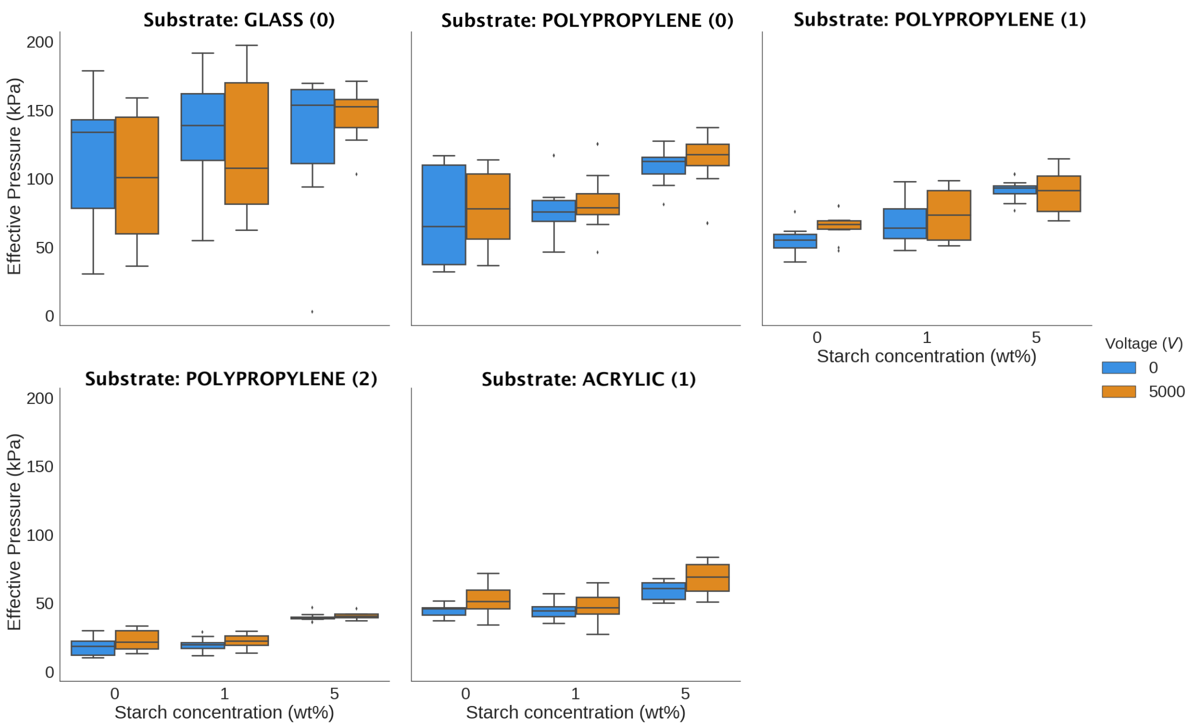

Figure 10: Results after effective surface correction on every non-MDF substrate for adhesive types #1, #2, and #3 with and without electrostatics.

References

[1] Mohammad Dadkhah, Donald Ruffatto III, Zhanyue Zhao, Matthew Spenko *Increasing adhesion via a new electrode design and improved manufacturing in electrostatic/microstructured adhesives*, Journal of Electrostatics 91 (2018) 48-55.

[2] S. Hirose, A. Nagakubo, R. Toyama, *Machine that can walk and climb on floors, walls and ceilings*, 5th International Conference on Advanced Robotics (1991) 753–758.

[3] W. Shen, J. Gu, Y. Shen, *Permanent magnetic system design for the wall-climbing robot*, July 2005, IEEE International Conference Mechatronics and Automation, vol. 4, 2005, pp. 2078–2083 vol. 4.

[4] A. Parness, M. Frost, N. Thatte, J.P. King, *Gravity-independent mobility and drilling on natural rock using microspines*, 2012 IEEE International Conference on Robotics and Automation (May 2012) 3437–3442.

[5] M. Henrey, J. Tellez, K. Wormnes, L. Pambaguian, C. Menon, *Sticking in space: manufacturing dry adhesives and testing their performance in space environments*, 12th Symposium on Advanced Space Technologies in Robotics and Automation, 2013.

[6] D. Ruffatto, A. Parness, M. Spenko, *Improving controllable adhesion on both rough and smooth surfaces with a hybrid electrostatic/gecko-like adhesive*, Journal of The Royal Society Interface 11 (no. 93) (2014) [Online]. Available http://rsif. royalsocietypublishing.org/content/11/93/20131089.

[7] M. Dadkhah, Z. Zhao, N. Wettels, M. Spenko, *A self-aligning gripper using an electrostatic/gecko-like adhesive*, 2016 IEEE/RSJ International Conference on Intelligent Robots and Systems (IROS), Oct 2016, pp. 1006–1011.

[8] J.C. Grieco, M. Prieto, M. Armada, P.G. de Santos, *A six-legged climbing robot for high payloads*, Proceedings of the 1998 IEEE International Conference on Control Applications (Cat. No.98CH36104), vol. 1, Sep 1998, pp. 446–450 vol. 1.

[9] H. Prahlad, R. Pelrine, S. Stanford, J. Marlow, R. Kornbluh, *Electroadhesive robots–wall climbing robots enabled by a novel, robust, and electrically controllable adhesion technology*, Proceedings of the IEEE International Conference on Robotics and Automation, 2008, pp. 3028–3033.

[10] M.A. Graule, P. Chirarattananon, S.B. Fuller, N.T. Jafferis, K.Y. Ma, M. Spenko, R. Kornbluh, R.J. Wood, *Perching and takeoff of a robotic insect on overhangs using switchable electrostatic adhesion*, Science vol. 352, (6288) (2016) 978–982.

[11] A. Kalantari, K. Mahajan, D. Ruffatto, M. Spenko, *Autonomous perching and take-off on vertical walls for a quadrotor micro air vehicle*, 2015 IEEE International Conference on Robotics and Automation (ICRA), May 2015, pp. 4669–4674.

[12] T. Debus, S. Dougherty, *Overview and perrformance of the front-end robotics enabling near-term demonstratiion (frend) robotic arm*, AIAA Aerospace Conference (2009) 461–465.

[13] G. Monkman, *Electroadhesive microgrippers*, Ind. Robot 30 (4) (2003) 326–330.

[14] G. Monkman, *An analysis of astrictive prehension*, Int. J. Robot Res. 16 (1) (1997) 1–10.

[15] D. Ruffatto, J. Shah, M. Spenko, *Increasing the adhesion force of electrostatic adhesives using optimized electrode geometery and a novel manufacturing process*, J. Electrost. 72 (2) (2014) 147–155.

[16] A. Geim, S. Dubonos, I. Grigorieva, K. Novoselov, A. Zhukov, S. Shapoval, *Microfabricated adhesive mimicking gecko foot-hair*, Nat. Mater. 2 (2003) 461–463.

[17] A. del Campo, E. Arzt, *Design parameters and current fabrication approaches for developing bioinspired dry adhesives*, Macromol. Biosci. 7 (2007) 118–127.

[18] A. Parness, *Microstructured Adhesives for Climbing Applications*, Stanford University Thesis (2010).

[19] D. Santos, M. Spenko, A. Parness, S. Kim, M. Cutkosky, *Directional adhesion for climbing: theoretical and practical considerations*, J. Adhes. Sci. Technol. 21 (12–13) (2007) 1317–1341.

[20] D. Ruffatto, J. Shah, M. Spenko, *Optimization of electrostatic adhesives for robotic climbing and manipulation*, Proceedings of the ASME 36th Mechanisms and Robotics Conference, 2012, pp. 1143–1152.

[21] *Optimization and experimental validation of electrostatic adhesive geometry*, IEEE Aerospace Conference, 2013.